Available online at www.sciencedirect.com

SciVerse ScienceDirect

Ceramics International 38 (2012) 1241–1247

CERAMICS INTERNATIONAL

www.elsevier.com/locate/ceramint

Preparation and indirect selective laser sintering of alumina/PA microspheres

Khuram Shahzad [a], Jan Deckers [b], Stijn Boury [b], Bram Neirinck [a], Jean-Pierre Kruth [b], Jef Vleugels [a,*]

[a] Department of Metallurgy and Materials Engineering, Katholieke Universiteit Leuven, Kasteelpark Arenberg 44, B-3001, Heverlee, Belgium
[b] Division PMA, Department of Mechanical Engineering, Katholieke Universiteit Leuven, Celestijnenlaan 300B, B-3001 Heverlee, Belgium

Received 29 July 2011; received in revised form 22 August 2011; accepted 23 August 2011
Available online 2 September 2011

Abstract

Indirect selective laser sintering (SLS) is a promising additive manufacturing technique to produce ceramic parts with complex shapes in a two-step process. In the first step, the polymer phase in a deposited polymer/alumina composite microsphere layer is locally molten by a scanning laser beam, resulting in local ceramic particle bonding. In the second step, the binder is removed from the green parts by slowly heating and subsequently furnace sintered to increase the density. In this work, polyamide 12 and submicrometer sized alumina were used. Homogeneous spherical composite powders in the form of microspheres were prepared by a novel phase inversion technique. The composite powder showed good flowability and formability. Differential scanning calorimetry (DSC) was used to determine the thermal properties and laser processing window of the composite powder. The effect of the laser beam scanning parameters such as laser power, scan speed and scan spacing on the fabrication of green parts was assessed. Green parts were subsequently debinded and furnace sintered to produce crack-free alumina components. The sintered density of the parts however was limited to only 50% of the theoretical density since the intersphere space formed during microsphere deposition and SLS remained after sintering.

Keywords: Additive manufacturing; Indirect selective laser sintering; Alumina; Polymer/ceramic microspheres

1. Introduction

Selective laser sintering (SLS) is a powder-based additive manufacturing (AM) process used to fabricate complex shaped parts without using preforms or moulds. As depicted in Fig. 1, a counter current roller or scraper system is conventionally used to deposit successive powder layers. A laser beam is used as a heating source for selectively sintering each powder layer according to predetermined geometries. The SLS process is vastly studied for polymeric and metallic materials, and different polymer and metal powders are commercially developed to produce fully functional parts [1]. Although SLS of ceramics was initiated in the beginning of the 1990s, the technology has not yet been commercialized due to the complexity of laser processing of ceramic powders. Ceramics generally have a very high melting point, low thermal shock resistance and low or no plasticity which makes them more challenging to SLS than polymers and metals.

Current commercial SLS equipment uses a roller or scraper to deposit powder layers. The starting powder should be free flowing, requiring a preferably spherical shape and size of ~50 μm [2]. To produce dense ceramic parts via solid state sintering on the other hand requires submicrometer sized starting powder. To achieve a high flowability, fine ceramic powders can be spray dried to produce spherical granules. Moreover, the layers produced by conventional SLS deposition systems are very porous [3], whereas a very good contact between the particles is required for solid state sintering [4]. In general, the classical roller deposition conditions are not favourable for solid state sintering and the parts produced are very fragile and porous [4,5]. Colloidal processing based techniques, such as tape casting and spray deposition, were studied to produce high density layers [6–8]. Although SLS of these higher density powder layers allowed production of dense

* Corresponding author. Tel.: +32 16 321244; fax: +32 16 321992.
E-mail address: jozef.vleugels@mtm.kuleuven.be (J. Vleugels).

0272-8842/$36.00
doi:10.1016/j.ceramint.2011.08.055

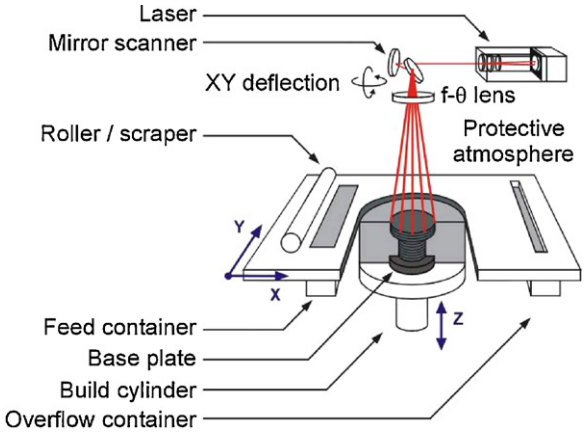

Fig. 1. Schematic of the SLS process.

microstructures, it was not possible to completely eliminate drying and thermal cracks [6–8]. Hagedorn et al. [9] used the selective laser melting (SLM) technique to produce dense Al_2O_3/ZrO_2 ceramic parts. To avoid thermal cracks, a preheating temperature >1600 °C was used. Although the produced parts were fully dense, the surface finish and accuracy was poor [9].

A two step indirect SLS process could be a good alternative to produce crack free parts. In the first step, green parts are produced in a layer by layer sequence by scanning with a laser beam targeting polymer phase melting and binding of the ceramic powder. In the second step, the binder is removed from the green parts by slowly heating prior to furnace sintering to increase the density. This approach so far did not get much attention because of the difficulties involved in the selection of a polymer binder phase and the preparation of homogeneous and free flowing composite powders. Gill et al. produced SiC/polyamide composite parts from blended composite powder [10]. The polyamide fraction was molten as a result of laser beam irradiation, gluing the SiC particles together [10]. The production of pure SiC parts by subsequent debinding and sintering however was not investigated. Subramanian et al. studied the SLS of alumina/polymer blends followed by infiltration in an attempt to increase the green part density [11]. The formability and strength of green parts obtained by indirect SLS of ball-milled alumina/polyamide powder was also reported to be poor [12].

In this work, polyamide 12 (PA 12), a semi-crystalline polymer is selected as binder phase. The phase inversion technique was adopted to produce homogeneous Al_2O_3–PA composite microspheres, allowing to use a conventional roller system for powder deposition. The influence of the polymer content and the SLS parameters on the green and sintered density of alumina parts produced by the indirect SLS/debinding/sintering process are assessed.

2. Experimental details

2.1. Materials

High purity α-alumina (grade SM8, Baikowski, France) powder with a $d_{50} \sim 0.3$ μm was used as a structural material and polyamide 12 (PA 12) (grade DuraForm PA, 3D Systems, USA) with a $d_{50} \sim 100$ μm was used as binder phase. Dimethyl sulfoxide (DMSO, Merck Co.) was used as solvent for the composite microsphere preparation.

2.2. Composite microsphere preparation

A schematic of the phase inversion process used to produce alumina-PA composite microspheres is given in Fig. 2. Alumina and PA powders (10 vol%) were added to DMSO (90 vol%) and the suspension was externally mechanically stirred in a 2 L flask. The suspension was heated to 140 °C (above the dissolution temperature ~135 °C) for 15 min under N_2 atmosphere to dissolve the PA in DMSO. The suspension was allowed to precipitate during natural cooling to room temperature. Vacuum filtration was used to separate the Al_2O_3–PA precipitates from the DMSO and around 80% of the DMSO was recovered and reused. The precipitates were subsequently washed multiple times with technical grade ethanol and dried in an oven at 80 °C for 24 h. Two compositions with 50 (CP50:50) and 40 (CP40:60) vol% alumina were produced. Combined differential scanning calorimetry (DSC) and thermal gravimetric analysis (TGA) (Model-2920, TA instruments, USA) was used to determine the thermal properties of the composite powder. The particle size of the composite microspheres was measured by laser diffraction (Mastersizer Plus, Malvern, UK), whereas the morphology was studied by scanning electron microscopy (SEM, XL30-FEG, FEI, The Netherlands).

2.3. Selective laser sintering process

Green samples were fabricated using a Sinterstation 2000 (DTM Corporation/3D Systems, USA) equipped with a 100 W CO_2 laser (f100, Synrad, USA) with a wavelength of 10.6 μm and a laser beam diameter $\varnothing_{1/e_2}$ of 400 μm. Powder layers were deposited by a counter current roller and irradiated with the laser beam. In order to avoid thermal oxidation of the PA, SLS was performed under N_2 atmosphere. All tests were performed by isothermally heating the powder bed at 160 °C, i.e., between the PA melting $T_m \sim 190$ °C and crystallization temperature $T_c \sim 157$ °C. The energy required to melt the PA was partially supplied by powder bed pre-heating and infra-red surface heating and partially by laser irradiation which locally raised the temperature above the melting point.

To produce green parts by indirect SLS, the machine and laser scanning parameters were tuned in such a way that the binder phase is locally heated between the melting and degradation temperature. In this study, the local temperature profile of the powder bed during laser irradiation was controlled by varying the laser power, P, the laser beam scan speed, v, and the laser beam scan spacing, s. The layer thickness, l, was kept constant. The laser energy density, e, combining these parameters is defined as:

$$e = \frac{P}{s.v.l} \quad (1)$$

In order to optimise the laser scanning parameters, multilayer parts with a simple square shape (15 × 15 mm^2)

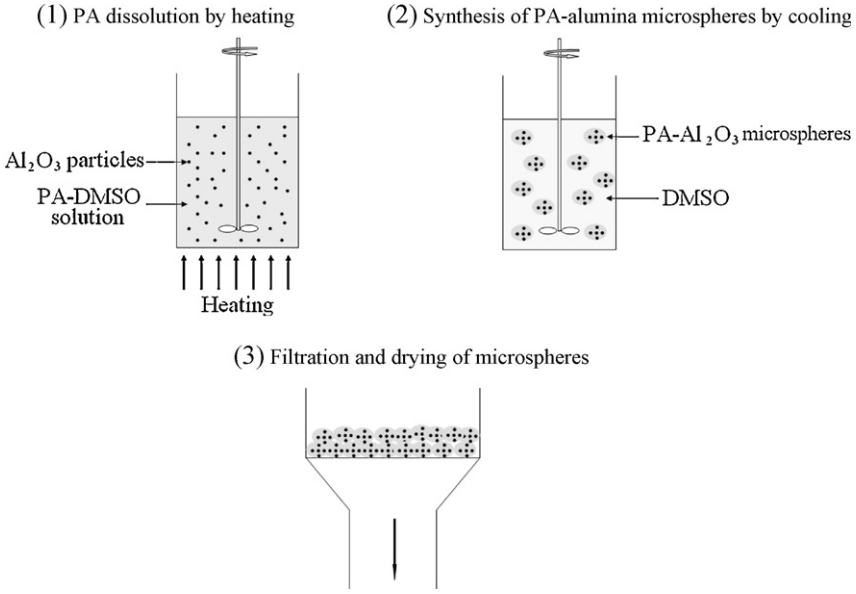

Fig. 2. Schematic of the composite microsphere production process.

were produced. The laser power (3, 5 and 7 watts), scan speed (100, 600 and 1257 mm/s) and scan spacing (150 and 300 μm) were varied at a constant deposited layer thickness of 150 μm. The density of the green parts was measured geometrically and the microstructure of fracture surfaces of the green parts was studied by SEM. The optimum parameters were used to build parts with complex shapes.

2.4. Post processing

The PA was removed from the green parts by slowly heating to 600 °C in air at a heating rate of 0.1 °C/min (Carbolite Furnace). After 2 h dwelling at 600 °C, the parts were slowly cooled down to room temperature. After binder removal, the parts were sintered at 1600 °C for 1 h in air at a heating rate of 5 °C/min (Nabertherm Furnace). The density of the parts was measured geometrically.

3. Results and discussion

3.1. Al_2O_3–PA agglomerate characteristics

Polymer–ceramic microspheres can be produced by a variety of techniques like suspension polymerization, immersion polymerization and phase inversion or dissolution-precipitation [13–15].

The phase inversion technique involves the dissolution of polymer in a suitable solvent by mixing, heating or increasing the pressure. The polymer is then allowed to precipitate from the homogeneous polymer solution by cooling the solution also known as thermally induced phase separation (TIPS), reducing the pressure, solvent evaporation or adding a non-solvent [16]. In this work, the TIPS technique was adopted because of its simplicity. Cooling of the polymer solution initiated a liquid-liquid phase separation forming a diluent rich phase and a polymer rich phase. Upon further cooling, the polymer rich phase solidifies and locks the morphology of the precipitated polymer. The morphology of the polymer after phase separation from a homogeneous polymer solution is schematically presented in Fig. 3. In the unstable region B, the phase separation initiated by spinodal decomposition will result in the formation of a bi-continuous membrane structure. In contrast, phase separation in the metastable A regions is initiated by binodal decomposition according to a nucleation and growth mechanism. In a dilute polymer solution with a polymer concentration below the critical concentration, polymer rich phase droplets nucleate and grow from of the polymer lean phase that forms the continuous matrix. The formation of spherical shape polymer particles is favoured. At a polymer concentration above the critical composition, droplets of

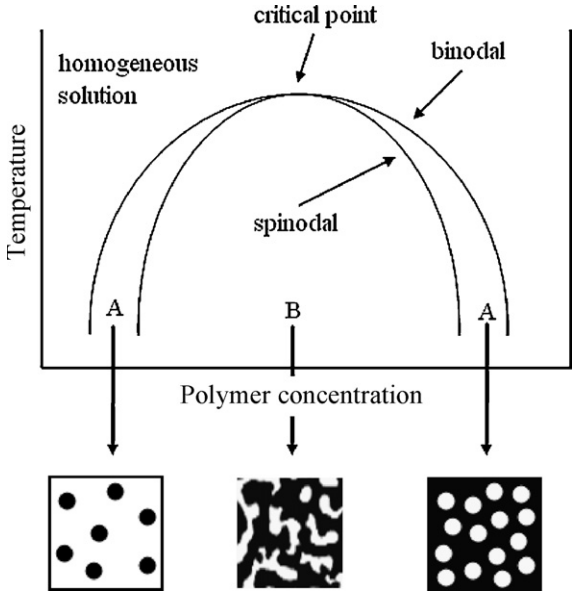

Fig. 3. Schematic phase diagram of a polymer solution and morphologies that can be obtained by thermally induced phase separation.

polymer lean phase separate from the polymer rich continuous matrix phase, resulting in the formation of cellular membrane structures. The phase separation in dilute polymer solutions containing suspended Al_2O_3 particles can result in the formation of composite polymer/ceramic microspheres.

SEM micrographs of the CP50:50 microspheres produced by TIPS, shown in Fig. 4, reveal that the alumina particles are efficiently engulfed by the polymer during the precipitation process. The composite powder shows a nice spherical shape in the 10–100 μm size range. The size of the CP50:50 and CP40:60 materials were assessed by laser diffraction, as presented in Fig. 5. The logarithmic distribution of CP50:50 shows two separate peaks. The major peak with an average sphere size of 52 μm containing 98.41 vol% ranged from 2 to 105 μm. The small peak ranging from 0.4 to 0.8 μm, containing only 1.59 vol% of the powder, corresponds to the size of the alumina starting powder and represents the fraction of alumina powder that is not encapsulated during the precipitation process. The CP40:60 powder shows a monomodal distribution with an average diameter of ∼53 μm and a particle size ranging from 2 to 105 μm. However, most of the particles range from 20 to 100 μm. These analyses recommend phase inversion/TIPS as a suitable technique to produce ceramic/polymer composite microspheres for indirect SLS applications.

To produce dense polymer parts, semi-crystalline polymers are preferred over amorphous polymers. Above the melting temperature, T_m, the semi-crystalline polymers exhibit a relatively low viscosity, as compared to amorphous polymers, which favours the rate and amount of consolidation. However, the solidification of the polymer results in a 5–7% shrinkage, a phenomenon not occurring in amorphous polymers, which may induce geometrical inaccuracies and distortion in the parts. Previous investigations on the laser sintering process of semi-crystalline thermoplastics led to the development of a process model for successful SLS of polymers, based on the so called quasi-isothermal selective laser sintering theory [17,18]. The processing of the polymer is performed at constant ambient temperature. Melting of the polymer is locally generated without increasing the temperature of the surrounding powder. The selective energy induced by the laser in combination with the high melting enthalpy and low thermal conductivity of the polymer avoids the fusion of adjacent particles. Due to the hysteresis between melting and crystallization temperature, molten areas coexist with solid powder over a long period of time, i.e., the liquid and solid phases coexist during the building process. After sintering all layers, the component containing powder bed is cooled homogeneously, limiting warpage of the produced parts [2,17,18].

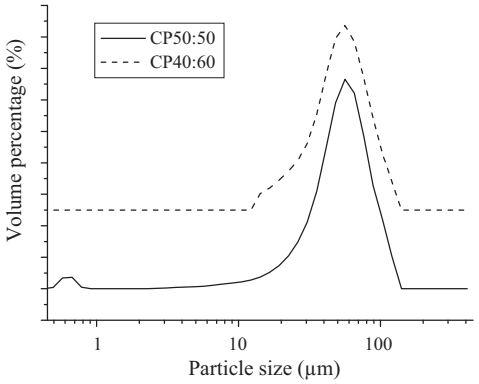

Fig. 5. Particle size distribution of CP50:50 and CP40:60 composite microspheres.

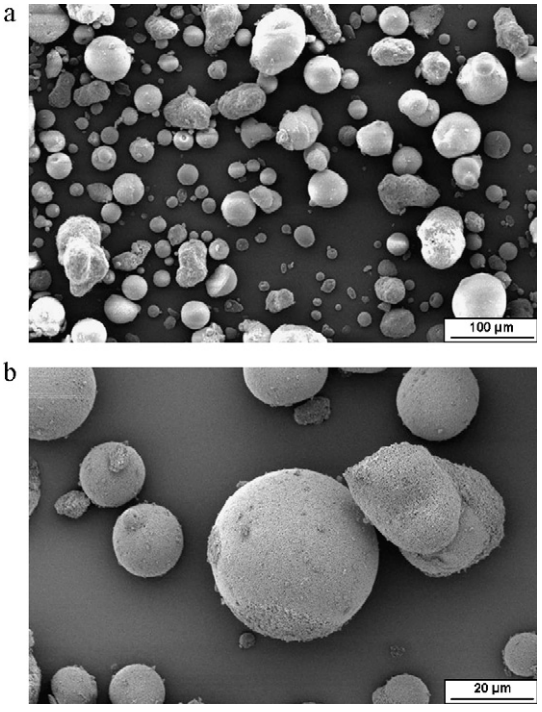

Fig. 4. SEM micrograph of the CP50:50 composite microspheres at low (a) and high (b) magnification.

To produce distortion free parts, the melting and crystallization behaviour of the polymer is extremely important. For polymers with a small difference in melting, T_m, and crystallization, T_c, temperature, it is difficult to avoid the distortion of parts during the building process [2]. Therefore, polymers with a substantially large difference in T_m and T_c ($T_m - T_c > 5\ ^\circ C$) are preferred. This temperature difference, ΔT, is also referred to as the SLS window and can be determined by the following equation.

$$\Delta T = T_{om} - T_c \quad (2)$$

where T_{om} is the onset melting temperature and T_c represents the onset temperature of crystallization. In this study, PA 12 was used as a binder phase. In the context of the discussion in the previous paragraphs, the transition temperatures of the composite powder should be known to determine the SLS conditions. The ΔT value of the composite microspheres and the PA starting powder were determined from the DSC curves, shown in Fig. 6, and are compared with that of pure PA in Table 1. Although the addition of alumina particles resulted in a slight increase of the melting and crystallization temperature and slight decrease in the SLS window, a substantially large SLS process window remained to avoid distortion of the parts.

3.2. Green part fabrication

Composite microspheres produced by TIPS of a PA solution showed excellent flowability and formability. Green parts could only be built in a narrow laser energy density window. Using a too high laser energy density resulted in the decomposition of PA and distortion of the parts. Applying a too low laser energy density resulted in very fragile parts with limited sintering. The green parts produced by SLS in the 0.176 and 0.37 J/mm^3 laser energy density range allowed manufacturing green parts with a strength allowing non-destructive manipulation of the green parts. The density and microstructure of the green parts are very important since they determine the sintered density and final microstructure. The effect of the laser energy density in the stable window range on the green density of the samples produced from the CP40:60 and CP50:50 composite microspheres is presented in Fig. 7. The green density of the parts increased with increasing laser energy density. The maximum density achieved by SLS of CP40:60 is 54.8% of the composite theoretical density (TD), which after debinding accounts for ~22% of the TD of Al_2O_3.

The parts produced from the CP40:60 grade showed higher green densities than those produced from CP50:50. An SEM image of a fracture surface of a green SLS CP50:50 part, shown in Fig. 8a, clearly shows that the spheres of the starting powder did not collapse during SLS, implying no plastic flow of the composite powder. Consequently, the residual intersphere space of the loose powder packing basically remains after SLS. In the part produced from CP40:60 (Fig. 8b) however, there is a clear indication of polymer and material flow during SLS, explaining the higher green density of the SLS CP40:60 material. The measured density is compared in Table 2.

Ideally, to produce dense parts during SLS, the powder should melt, flow and make a dense and continuous film on the previously sintered layer. The addition of the fine alumina particles to PA however increased the melt viscosity of PA and did not allow a sufficient melt flow, indicating that the melt viscosity of the composite powder is a crucial parameter. The melt viscosity of the composite powder can be decreased by decreasing the molecular weight of the polymer, decreasing the ceramic loading, increasing the particle size of the ceramic powder, or by adding a plasticizer to the polymer [19–21]. At present, the relation between the melt viscosity of the composite powder and the green density of the parts produced by SLS is unknown and is the focus of future research. Additional efforts should be made to investigate the rheological properties of the ceramic-binder formulation and find the optimum composition which can provide a suitable melt viscosity to achieve high densities and shape retention during SLS as well as polymer debinding step.

Table 1
Transition temperatures of the PA DuraForm and CP50:50 and CP40:60 composite microspheres.

Powder	T_{om} (°C)	T_{mp} (°C)	T_c (°C)	$\Delta T = T_{om} - T_c$ (°C)
PA Dura form	180.6	186.3	152.8	27.8
CP40:60	184.2	190.2	156.9	27.3
CP50:50	184.1	189.6	157.5	26.6

T_{om} = melting onset temperature; T_{mp} = melting peak temperature; T_c = crystallization temperature; ΔT = SLS window.

3.3. Post-processing of green parts

Prior to furnace sintering, the PA was removed from the green parts by thermal decomposition in air. The heating rate is a key parameter in the debinding process and should be carefully controlled. The PA weight loss curve (TGA) in air at a heating rate of 10 °C/min is shown in Fig. 9. The onset of weight loss starts around 290 °C, with a complete debinding at ~590 °C. Binder removal of the green parts was successfully performed by heating the SLS parts to 600 °C at a heating rate of 0.1 °C/min. After binder removal, the parts were visually inspected and no cracks or distortion of the samples were observed.

After binder removal, the green parts were sintered in air at 1600 °C for 60 min. During sintering, the parts showed a homogeneous volume shrinkage of around 20%. As shown in Table 2, the green and sintered density of the CP40:60 is higher than for CP50:50, despite the 10 vol% higher polymer content of CP40:60. The reason for this is the plastic flow of the

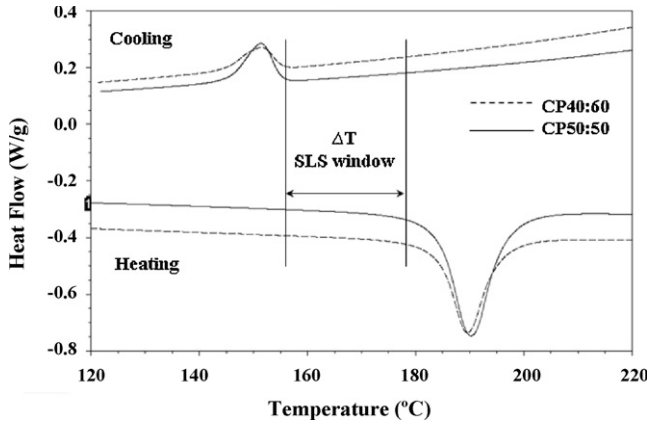

Fig. 6. DSC measurement of the CP50:50 and CP40:60 composite microspheres.

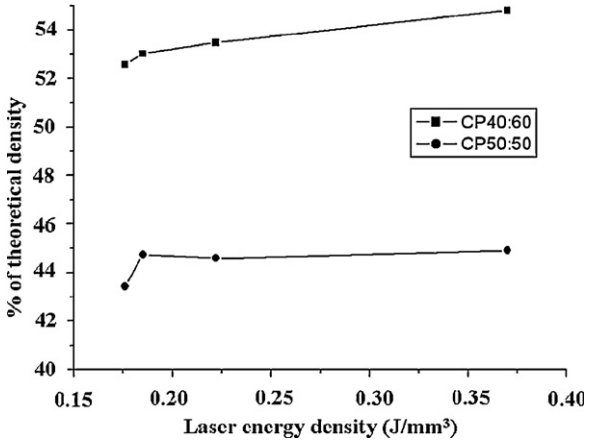

Fig. 7. Effect of laser energy density on the density of the green PA–Al_2O_3 composite parts.

Table 2
Green and sintered densities of the parts produced from CP40:60 and CP50:50 powders.

Starting powder	SLS parameters	Green density g/cm^3 (%TD)[a]	Green density (after binder removal) g/cm^3 (%TD)[b]	Sintered density g/cm^3 (%TD)[b]
CP40:60	P = 5 W v = 600 mm/s s = 150 μm l = 150 μm	1.28 (54.8%)	0.92 (23.4%)	2.01 (50.4%)
CP50:50		1.12 (44.9%)	0.90 (22.9%)	1.72 (43.1%)

[a] Theoretical density of the composite.
[b] Theoretical density of Al_2O_3.

polymer during SLS of CP40:60, increasing the intersphere contact area after SLS and concomitantly larger Al_2O_3 interagglomerate neck size during sintering. The final density however is still modest, ranging from 50% for CP40:60 to 43% for CP50:50. The residual porosity is directly related to the intersphere space during SLS, which remains in the final microstructure as shown in Fig. 10 for the CP40:60 grade. To homogenize the sintered microstructure, the green SLS microstructure must be homogenized first by controlling the flow properties of the composite spheres and laser scanning parameters. Despite the high residual open porosity, it was possible to prepare complex shaped parts by the SLS/debinding/sintering process, as illustrated in Fig. 11.

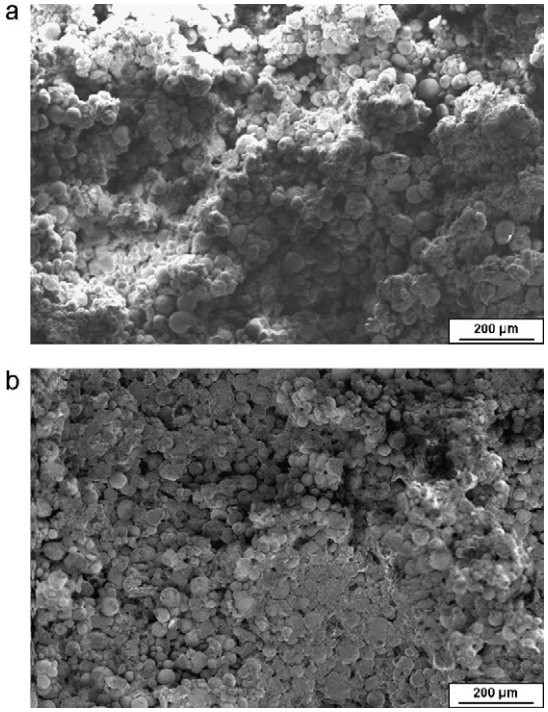

Fig. 8. SEM micrographs of fracture surfaces of green SLS CP50:50 (a) and CP40:60 (b) parts.

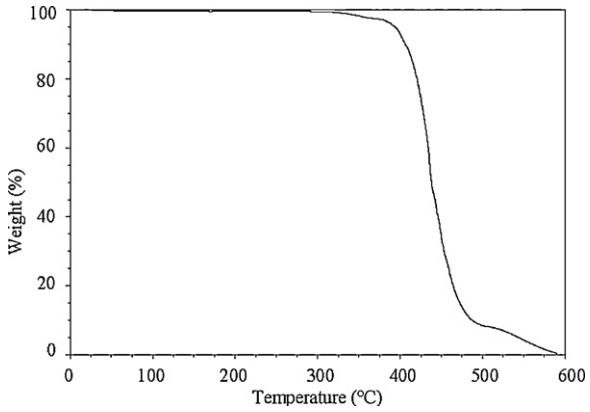

Fig. 9. TGA curve of DuraForm PA.

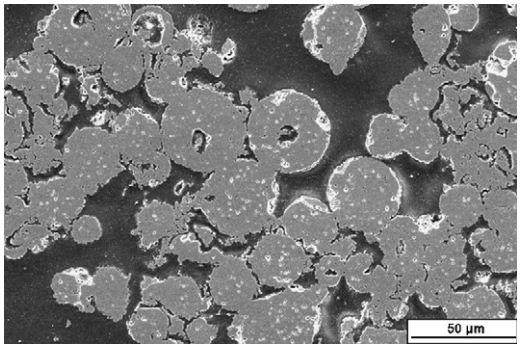

Fig. 10. SEM micrograph of the sintered ceramic.

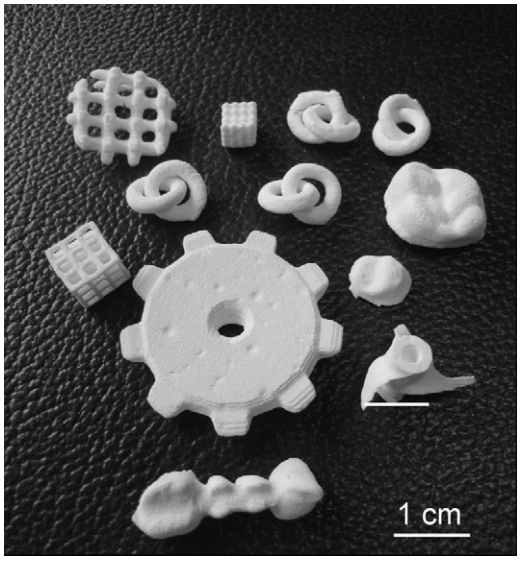

Fig. 11. Alumina parts fabricated by the SLS/debinding/sintering process.

4. Conclusions

Al_2O_3–polyamide microspheres with an average diameter of 50 μm could be fabricated by means of the phase inversion technique using DMSO as a solvent. These microspheres were successfully deposited by a conventional roller system during SLS.

The deposit layers could be SLS into components in the laser energy density range between 0.176 and 0.37 J/mm^3. At lower energies, the parts distorted whereas the PA burned at higher energy inputs. The green and sintered density of the starting material with 40 vol% Al_2O_3 was higher than for the 50 vol% Al_2O_3 material, due to the limited but observed plastic material flow during SLS of the higher PA content material. The sintered density of the Al_2O_3 ceramics however was limited to only 50% of the theoretical density since the intersphere space formed during microsphere deposition and SLS remained after sintering.

Despite the limited density, the sequence of SLS, debinding and sintering of ceramic–polymer microspheres, obtained by solution-reprecipitation, as an additive manufacturing technique for ceramics was proven to be feasible and promising, allowing to already manufacture crack-free complex shape components.

Acknowledgements

This work was financially supported by the Flemish Institute for the Promotion of Scientific Technological Research in Industry (IWT) under project SBO-DiRaMaP. B. Neirinck thanks the Research Fund of K.U. Leuven for his post-doctoral mandate and the Fund for Scientific Research Flanders (FWO) for his post-doctoral fellowship.

References

[1] J.-P. Kruth, G. Levy, F. Klocke, T.H.C. Childs, Consolidation phenomena in laser and powder-bed based layered manufacturing, CIRP Annals–Manufacturing Technology 56 (2007) 730–759.
[2] J.E.D. Dickens, B.L. Lee, G.A. Taylor, A.J. Magistro, H. Ng, K.P. McAlea, P.F. Forderhase, Sinterable semi-crystalline powder and near-fully dense article formed therewith, US Patent RE39354E.
[3] S. Kolosov, G. Vansteenkiste, N. Boudeau, J.C. Gelin, E. Boillat, Homogeneity aspects in selective laser sintering (SLS), Journal of Materials Processing Technology 177 (2006) 348–351.
[4] M.N. Rahaman, Ceramic Processing and Sintering, Marcel Dekker, New York, 1995.
[5] Ph. Bertrand, F. Bayle, C. Combe, P. Goeuriot, I. Smurov, Ceramic component manufacturing by selective laser sintering, Applied Surface Science 254 (2007) 989–992.
[6] F. Klocke, C. Derichs, C. Ader, A. Demmer, Investigations on laser sintering of ceramic slurries, Production Engineering Research and Development 1 (2007) 279–284.
[7] Y. Wu, J. Du, K.-L. Choy, L.L. Hench, Laser densification of powder beds generated using aerosol assisted spray deposition, Journal of the European Ceramic Society 27 (2007) 4727–4735.
[8] A. Gahler, J.G. Heinrich, Direct laser sintering in the Al_2O_3–SiO_2 dental ceramic components by layer-wise slurry deposition, Journal of the American Ceramic Society 89 (2006) 3076–3080.
[9] Y. Hagedon, J. Wilkes, W. Meiners, K. Wissenbach, R. Poprawe, Net shaped high performance oxide ceramic by selective laser melting, Physics Proceedia 5 (2010) 587–594.
[10] T.J. Gill, K.K.B. Hon, Experimental investigations into the selective laser sintering of silicon carbide polyamide composites, Proceedings of the Institution of Mechanical Engineers: Part B Journal of Engineering Manufacture 218 (2004) 1249–1256.
[11] K. Subramanian, N. Vail, J. Barlow, H. Marcus, Selective laser sintering of alumina with polymer binders, Rapid Prototyping Journal 1 (1995) 24–35.
[12] J. Deckers, K. Shahzad, J. Vleugels, J.P. Kruth, Cold/quasi isostatic pressing assisted indirect selective laser sintering of alumina components, Journal of Rapid Prototyping, in Press.
[13] Q. Yuan, R.A. Williams, Large scale manufacture of magnetic polymer particles using membranes and microfluidic devices, China Particuology 5 (2007) 26–42.
[14] S. Freiberg, X.X. Zhu, Review: polymer microspheres for controlled drug release, International Journal of Pharmaceutics 282 (2004) 1–18.
[15] H. Kawaguchi, Functional polymer microspheres, Progress in Polymer Science 25 (2000) 1171–1210.
[16] P. Van de Witte, P.J. Dijkstra, J.W.A. Van den Berg, J. Feijen, Review: phase separation processes in polymer solutions in relation to membrane formation, Journal of Membrane Science 117 (1996) 1–31.
[17] B. Wendel, D. Rietzel, F. Kühnlein, R. Feulner, G. Hulder, E. Schmachtenberg, Review: additive manufacturing of polymers, Macromolecular Materials and Engineering 293 (2008) 799–809.
[18] D. Drummer, D. Rietzel, F. Kühnlein, Development of a characterization approach for the sintering behavior of new thermoplastics for selective laser sintering, Physics Procedia 5 (2010) 533–542.
[19] M.J. Edirisinghe, R.G. Evans, Review: fabrication of engineering ceramics by injection moulding. I. Materials selection, International Journal of High Technology Ceramics 2 (1986) 1–31.
[20] D.-M. Liu, Control of yield stress in low-pressure injection molding, Ceramics International 25 (1999) 587–592.
[21] Z.Y. Liu, N.H. Loh, S.B. Tor, K.A. Khor, Y. Murakoshi, R. Maeda, Bindre system for micropowder injection molding, Materials Letter 48 (2001) 31–38.